Dynamical matrix of two-dimensional electron crystals

R. Côté,[1] M.-A. Lemonde,[1] C. B. Doiron,[2] and A. M. Ettouhami[3]
[1]*Département de Physique and RQMP, Université de Sherbrooke, Sherbrooke, Québec, Canada J1K 2R1*
[2]*Department of Physics, University of Basel, Klingelbergstrasse 82, CH-4056 Basel, Switzerland*
[3]*Department of Physics, University of Toronto, 60 St. George Street, Toronto, Ontario, Canada M5S 1A7*
(Received 11 June 2007; revised manuscript received 12 February 2008; published 3 March 2008)

In a quantizing magnetic field, the two-dimensional electron gas has a rich phase diagram with broken translational symmetry phases such as Wigner, bubble, and stripe crystals. In this paper, we derive a method to obtain the dynamical matrix of these crystals from a calculation of the density response function performed in the generalized random-phase approximation (GRPA). We discuss the validity of our method by comparing the dynamical matrix calculated from the GRPA with that obtained from standard elasticity theory with the elastic coefficients obtained from a calculation of the deformation energy of the crystal.

DOI: 10.1103/PhysRevB.77.115303 PACS number(s): 73.20.Qt, 73.21.−b, 73.43.−f

I. INTRODUCTION

Theoretical calculations show that, in the presence of a perpendicular magnetic field, a two-dimensional electron gas (2DEG) should crystallize below a filling factor $\nu \sim 1/6.5$.[1] Several experimental groups have reported transport measurements indicative of this electron crystallization when the filling factor of the lowest Landau level is decreased below $\nu=1/5$. These measurements include the observation of a strong increase in the diagonal resistivity ρ_{xx}, nonlinear *I-V* characteristics, and broadband noise. All these observations have been interpreted as the pinning and sliding of a Wigner crystal (WC).[2] Moreover, microwave absorption experiments[3] have also detected a resonance in the real part of the longitudinal conductivity, $\sigma_{xx}(\omega)$, that has been attributed to the pinning mode of a disordered Wigner crystal. The vanishing of the pinning mode resonance at some critical temperature $T_m(\nu)$ has been used to derive the phase diagram of the crystal[4] in the quantum regime where the kinetic energy is frozen by the quantizing magnetic field. Similar microwave absorption experiments also showed a pinning resonance at higher filling factors close to $\nu=1,2,3$, where the formation of a Wigner solid is expected in very clean samples.[5–7] Finally, in Landau levels of index $N>1$, a study of the evolution of the pinning mode with filling factor reveals several transitions of the 2DEG ground state from a Wigner crystal at low ν to bubble crystals with increasing number of electrons per lattice site as ν is increased and into a modulated stripe state (or anisotropic Wigner crystal) near half-filling.[8]

In earlier works,[9,12] some of us have studied several crystalline states of the 2DEG using a combination of Hartree–Fock approximation (HFA) and generalized random-phase approximation (GRPA). In these works, the energy and order parameters of the crystal were calculated in a self-consistent HFA, while the collective excitations were derived from the poles of density response functions computed in the GRPA. This microscopic approach (HFA+GRPA) works well at zero temperature but is difficult to generalize to consider finite-temperature effects or to include quantum fluctuations beyond the GRPA. Finite-temperature or quantum fluctuation effects (not already included in the GRPA) are most easily computed by writing down an elastic action for the system. For a crystalline solid, this requires the knowledge of the dynamical matrix (DM) or, equivalently, of the elastic coefficients of the solid.

A direct way to obtain these elastic coefficients is to compute the energy required for various static deformations of the crystal. Using elasticity theory, each deformation energy ΔE_i can be written in the form $\Delta E_i=\frac{1}{2}C_i u_0^2$, where u_0 is a parameter characterizing the amplitude of the deformation and C_i is generally a combination of elastic constants. In the limit $u_0 \to 0$, one can obtain the elastic coefficients by computing the deformation energy of one or more static deformations and using the known symmetry relations between the elastic constants. Alternatively, one can obtain a DM from the GRPA density response function much more directly without the need to compute the elastic coefficients.[10]

In this paper, we compare the DM obtained from these two methods (deformation energy and GRPA) in order to find the range of validity as well as the limitations of the GRPA approach. We first consider the simple case of an isotropic (triangular) Wigner crystal before tackling the more complex anisotropic Wigner crystal[12] or stripe phase that occurs near half-filling in the higher Landau levels. We show that although the GRPA method gives a good description of the qualitative behavior of the DM as a function of filling factor, its quantitative predictions must be used with caution. As we will show below, an averaging procedure must be applied to the method in order to obtain a DM in the GRPA that compares favorably with the one obtained by computing the deformation energy.

Our paper is organized as follows. In Sec. II, we define the elastic constants needed to build an elastic model for the Wigner and stripe crystals. We then explain in Sec. III how these elastic constants can be derived by computing the deformation energy of the crystals in the HFA. In Sec. IV, we summarize the GRPA method of obtaining the dynamical matrix. Our numerical results for the WC are discussed in Sec. V and those for the stripe crystal in Sec. VI. Section VI contains our conclusions.

II. ELASTIC CONSTANTS AND DYNAMICAL MATRIX

We describe the elastic deformation of a crystal state by a displacement field $\mathbf{u}(\mathbf{R})$ defined on each lattice site $\mathbf{R}$. The

 ©2008 The American Physical Society

Fourier transform of this operator is given by

$$\mathbf{u}(\mathbf{k}) = \frac{1}{\sqrt{N_s}} \sum_{\mathbf{R}} e^{-i\mathbf{k}\cdot\mathbf{R}} \mathbf{u}(\mathbf{R}), \tag{1}$$

where N_s is the number of lattice sites. In two dimensions, the general expression for the deformation energy of a crystal requires the use of six elastic coefficients c_{ij} and is given in the continuum limit by the following expression:[11]

$$\Delta E = \frac{1}{2} \int d\mathbf{r} [c_{11} e_{x,x}^2 + 4c_{66} e_{x,y}^2 + 4c_{62} e_{x,y} e_{yy}] + \frac{1}{2} \int d\mathbf{r} [2c_{12} e_{x,x} e_{y,y} + 4c_{16} e_{x,x} e_{x,y} + c_{22} e_{y,y}^2], \tag{2}$$

where

$$e_{\alpha,\beta}(\mathbf{r}) = \frac{1}{2} \left(\frac{\partial u_\alpha(\mathbf{r})}{\partial r_\beta} + \frac{\partial u_\beta(\mathbf{r})}{\partial r_\alpha} \right) \tag{3}$$

is the symmetric strain tensor.

The Wigner and bubble crystals have a triangular lattice structure for which the following equation holds:

$$c_{11} = c_{22} = 2c_{66} + c_{12}. \tag{4}$$

For such a triangular structure, the elastic energy in the long-wavelength limit can be written in a form that contains only two elastic coefficients, namely,

$$\Delta E = \frac{1}{2} \int d\mathbf{r} [c_{12}(e_{x,x}^2 + e_{y,y}^2 + 2e_{x,x}e_{y,y}) + 2c_{66}(e_{x,x}^2 + e_{y,y}^2 + 2e_{x,y}^2)]. \tag{5}$$

The anisotropic stripe state can be seen either as a centered rectangular lattice with two electrons per unit cell or as a rhombic lattice with one electron per unit cell with reflection symmetry in both the x and y axes. The deformation energy is given by

$$\Delta E = \frac{1}{2} \int d\mathbf{r} [c_{11} e_{x,x}^2 + 4c_{66} e_{x,y}^2] + \frac{1}{2} \int d\mathbf{r} [2c_{12} e_{x,x} e_{y,y} + c_{22} e_{y,y}^2]. \tag{6}$$

In this paper, we assume that the stripes are aligned along the y axis.

The above formulation of elasticity theory assumes short-range forces only. For the electronic crystals that we consider, these forces are of Coulombic origin, i.e., the Hamiltonian of the crystal contains only the Coulomb interaction between electrons and the kinetic energy which is frozen by the quantizing magnetic field. Both the direct (Hartree) and exchange (Fock) terms are considered by the Hartree–Fock approximation as we will explain in the next section. To take into account the long-range part of the Coulomb interaction present in a crystal of electrons in the elasticity theory, it is necessary to add to ΔE the deformation energy ΔE_C given by

$$\Delta E_C = \frac{e^2}{2} \int d\mathbf{r} \int d\mathbf{r}' \frac{\delta n(\mathbf{r}) \delta n(\mathbf{r}')}{\kappa |\mathbf{r} - \mathbf{r}'|} = \frac{\pi e^2}{S} \sum_{\mathbf{q}} \frac{\delta n(\mathbf{q}) \delta n(-\mathbf{q})}{\kappa q}, \tag{7}$$

where S is the area of the crystal, $\delta n(\mathbf{q}) = \int d\mathbf{r} e^{-i\mathbf{q}\cdot\mathbf{r}} \delta n(\mathbf{r})$ is the Fourier transform of the change in the electronic density, and κ is the dielectric constant of the host semiconductor. We consider the positive background of ionized donors as homogeneous and inert, so that no linear term in $\delta n(\mathbf{r})$ is introduced by the Coulomb interaction.

To define a dynamical matrix, we assume that the crystal can be viewed as a lattice of electrons with static form factor $h(\mathbf{r})$ on each crystal site [with the normalization $\int d\mathbf{r} h(\mathbf{r}) = 1$]. The time-dependent density can then be written as

$$n(\mathbf{r}, t) = \sum_{\mathbf{R}} h[\mathbf{r} - \mathbf{R} - \mathbf{u}(\mathbf{R}, t)], \tag{8}$$

and, to first order in the displacement field, we have the following for a density fluctuation:

$$\delta n(\mathbf{k} + \mathbf{G}, t) = -ih(\mathbf{k} + \mathbf{G}) \sqrt{N_s} (\mathbf{k} + \mathbf{G}) \cdot \mathbf{u}(\mathbf{k}, t), \tag{9}$$

where $\mathbf{G}$ is a reciprocal lattice vector and $\mathbf{k}$ a vector in the first Brillouin zone of the crystal. It follows that we can write the Coulomb energy as

$$\Delta E_C = \pi n_0 e^2 \sum_{\mathbf{q}} \frac{|h(\mathbf{q}) \mathbf{q} \cdot \mathbf{u}(\mathbf{q})|^2}{\kappa q}, \tag{10}$$

where $n_0 = N_s / S$ is the average electronic density.

We pause at this point to remark that the form factor $h(q) \sim e^{-q^2 \ell^2/2}$ (with $\ell = \sqrt{\hbar c / eB}$ the magnetic length, B being the applied magnetic field) in Eq. (10) renders the summation over the wave vectors rapidly convergent. Our Hartree–Fock calculation of the ground-state energy of the electronic crystals, as well as our GRPA calculation of the dynamical matrix, also involves summations over reciprocal lattice vectors $\mathbf{G}$ of some functions weighted by $h(G)$. If the magnetic field is not too strong, we can perform these summations directly. There is no need to use Ewald's summation technique, as is the case if one works with a crystal of point electrons. Of course, as the filling factor $\nu \to 0$, the magnetic length $\ell \to 0$, so the electrons behave more and more like point particles and the convergence is lost. In all cases that we consider, the summations involved are rapidly convergent because we restrict ourselves to filling factors $\nu = 2\pi n_0 \ell^2 \gtrsim 0.1$ where ℓ / a_0 is sufficiently large for $e^{-G^2 \ell^2/2}$ to be small (a_0 being the lattice constant). The cutoff in G is chosen, so that the summations are evaluated with the required degree of accuracy.

The total deformation energy, which we now write as ΔE_T, now includes the long-range Coulomb interaction and can be written in the form

$$\Delta E_T = \frac{1}{2} \sum_{\mathbf{k}} u_\alpha(\mathbf{k}) D_{\alpha,\beta}(\mathbf{k}) u_\beta(-\mathbf{k}), \tag{11}$$

where we have introduced the dynamical matrix

$$D_{\alpha,\beta}(\mathbf{k}) = \frac{\partial^2 \Delta E_T}{\partial u_\alpha(\mathbf{k}) \partial u_\beta(-\mathbf{k})}. \tag{12}$$

For the triangular lattice, a comparison of Eqs. (11) and (5) gives the dynamical matrix (to order k^2) as

$$D_{x,x}(\mathbf{k}) = n_0^{-1}\{[\tilde{c}_{12}(k) + 2c_{66}]k_x^2 + c_{66}k_y^2\}, \tag{13a}$$

$$D_{x,y}(\mathbf{k}) = n_0^{-1}[\tilde{c}_{12}(k) + c_{66}]k_x k_y, \tag{13b}$$

$$D_{y,y}(\mathbf{k}) = n_0^{-1}\{[\tilde{c}_{12}(k) + 2c_{66}]k_y^2 + c_{66}k_x^2\}. \tag{13c}$$

The long-range Coulomb interaction renders the elastic coefficient c_{12} (but not the shear modulus c_{66}) nonlocal, so that c_{12} contains a diverging term $\sim 1/k$. We shall write

$$\tilde{c}_{12}(k) = \frac{2\pi n_0^2 e^2}{\kappa k} + c_{12}, \tag{14}$$

where c_{12} is the weakly dispersive part of the elastic coefficient and where the plasmonic (first) term on the right hand side is due to the long-range nature of the Coulomb interaction.

For the stripe state, Eq. (4) is no longer valid. In addition, all three elastic coefficients c_{11}, c_{12}, c_{22} become nonlocal. We have the following in this case:

$$D_{x,x}(\mathbf{k}) = n_0^{-1}[\tilde{c}_{11}(k)k_x^2 + c_{66}k_y^2] + n_0^{-1}Kk_y^4, \tag{15a}$$

$$D_{x,y}(\mathbf{k}) = n_0^{-1}[\tilde{c}_{12}(k) + c_{66}]k_x k_y, \tag{15b}$$

$$D_{y,y}(\mathbf{k}) = n_0^{-1}[\tilde{c}_{22}(k)k_y^2 + c_{66}k_x^2], \tag{15c}$$

where $\tilde{c}_{ij} = \frac{2\pi n_0^2 e^2}{\kappa k} + c_{ij}$, with $i,j = 1,2$, and where we added a term Kk_y^4 to $D_{x,x}(\mathbf{k})$ in order to take into account the bending rigidity of the stripes which, due to the small value of the shear modulus c_{66} in these systems, is quantitatively important over a sizable region of the Brillouin zone.[12] Using the fact that $n_0 = \nu/2\pi\ell^2$, we finally obtain

$$\tilde{c}_{ij} = \left(\frac{e^2}{\kappa\ell}\right)\frac{\nu}{k\ell}n_0 + c_{ij}. \tag{16}$$

We now want to discuss how one can evaluate the nondispersive part c_{ij} of the elastic coefficients. This will be the subject of the following section.

III. CALCULATION OF THE ELASTIC COEFFICIENTS IN THE HARTREE–FOCK APPROXIMATION

In the Hartree–Fock approximation, a crystalline phase is described by the Fourier components $\langle n(\mathbf{G})\rangle$ of the average electronic density, where $\mathbf{G}$ is a reciprocal lattice vector. In the strong magnetic field limit where the Hilbert space is restricted to one Landau level, it is more convenient to work with the "guiding-center density" $\langle \rho(\mathbf{G})\rangle$ which is related to $\langle n(\mathbf{G})\rangle$ by

$$\langle n(\mathbf{G})\rangle = N_\varphi F_N(\mathbf{G})\langle \rho(\mathbf{G})\rangle, \tag{17}$$

where N_φ is the Landau-level degeneracy and

$$F_N(\mathbf{G}) = e^{-G^2\ell^2/4} L_N^0\left(\frac{G^2\ell^2}{2}\right) \tag{18}$$

is the form factor of an electron in Landau level N [$L_N^0(x)$ being a generalized Laguerre polynomial]. The magnetic field $\mathbf{B} = B\hat{\mathbf{z}}$ is perpendicular to the 2DEG.

The Hartree–Fock energy per electron in the partially filled Landau level is given by[9,12]

$$\frac{E}{N_e} = \frac{1}{2\nu}\sum_{\mathbf{G}} [H(\mathbf{G})(1 - \delta_{\mathbf{G},0}) - X(\mathbf{G})]|\langle \rho(\mathbf{G})\rangle|^2, \tag{19}$$

where the $\delta_{\mathbf{G},0}$ term in this equation accounts for the neutralizing background of the ionized donors. The parameter $\nu = N_e/N_\varphi$ is the filling factor of the partially filled level, and we take all filled levels below N to be inert. The Hartree and Fock interactions in Landau level N are defined by

$$H(\mathbf{q}) = \left(\frac{e^2}{\kappa\ell}\right)\frac{1}{q\ell}e^{-q^2\ell^2/2}\left[L_N^0\left(\frac{q^2\ell^2}{2}\right)\right]^2, \tag{20a}$$

$$X(\mathbf{q}) = \left(\frac{e^2}{\kappa\ell}\right)\sqrt{2}\int_0^\infty dx e^{-x^2}[L_N^0(x^2)]^2 J_0(\sqrt{2}xq\ell), \tag{20b}$$

where $J_0(x)$ is the Bessel function of the first kind.

To compute the $\langle \rho(\mathbf{G})\rangle$'s, we first write this quantity in second quantization and in the Landau gauge $\mathbf{A} = (0, Bx, 0)$ as

$$\langle \rho(\mathbf{G})\rangle = \frac{1}{N_\varphi}\sum_X e^{-iG_x X + iG_x G_y \ell^2/2}\langle c_{N,X}^\dagger c_{N,X-G_y\ell^2}\rangle. \tag{21}$$

The average values $\langle \rho(\mathbf{G})\rangle$ are obtained by computing the single-particle Green's function (here and in what follows, T_τ denotes the time ordering operator):

$$G(X,X',\tau) = -\langle T_\tau c_{N,X}(\tau)c_{N,X'}^\dagger(0)\rangle, \tag{22}$$

whose Fourier transform we define as

$$G(\mathbf{G},\tau) = \frac{1}{N_\phi}\sum_{X,X'} e^{-(i/2)G_x(X+X')}\delta_{X,X'-G_y\ell^2}G(X,X',\tau), \tag{23}$$

so that

$$\langle \rho(\mathbf{G})\rangle = G(\mathbf{G},\tau = 0^-). \tag{24}$$

We use an iterative scheme to solve numerically[9] the Hartree–Fock equation of motion for $G(\mathbf{G},\tau)$. For the undeformed lattice, we use the basis vectors

$$\mathbf{R}_1 = a_0\eta\sin(\varphi)\hat{\mathbf{x}} + a_0\eta\cos(\varphi)\hat{\mathbf{y}}, \tag{25a}$$

$$\mathbf{R}_2 = a_0\hat{\mathbf{y}}, \tag{25b}$$

where η is the aspect ratio and φ is the angle between the two basis vectors. For the triangular lattice, $\eta = 1$ and $\varphi = \pi/3$. If we apply an elastic deformation $\mathbf{u}(\mathbf{r})$ to the lattice, the new lattice vectors are given by $\mathbf{R}' = n\mathbf{R}_1 + m\mathbf{R}_2 + \mathbf{u}(\mathbf{r})$ (where n,m are integers). We can write this expression as $\mathbf{R}' = n\mathbf{R}_1' + m\mathbf{R}_2'$ if we define the new basis vectors as

$$\mathbf{R}_1' = a_0'\eta' \sin(\varphi')\hat{\mathbf{x}} + a_0'\eta' \cos(\varphi')\hat{\mathbf{y}}, \tag{26a}$$

$$\mathbf{R}_2' = a_0'\hat{\mathbf{y}}. \tag{26b}$$

The parameters a_0', η', and φ' are functions of the original lattice and of the type of deformation considered. The reciprocal lattice vectors of the deformed lattice are easily computed once these parameters are known. Then, the cohesive energy $E(u_0)$ of the deformed lattice can be calculated using the deformed reciprocal lattice vectors and Eq. (9). Under these circumstances, we find that the deformation energy per electron is given by

$$f = \frac{E(u_0)}{N_e} - \frac{E(u_0=0)}{N_e}. \tag{27}$$

To find the elastic coefficients for the Wigner and stripe crystals, we need to consider the following deformations (note that the magnetic field and the number of electrons are kept fixed[12,13]):

(*i*) *A shear deformation with* $u_x(\mathbf{r})=u_0 y$ *and* $u_y(\mathbf{r})=0$. The strain tensors in this case are given by $e_{x,x}(\mathbf{r})=e_{y,y}(\mathbf{r})=0$ and $e_{x,y}(\mathbf{r})=u_0/2$. The area of the system, S, is not changed by this deformation and the elastic energy is given by $F_{shear}=\frac{1}{2}Sc_{66}u_0^2$. It then follows that the shear modulus c_{66} is given by

$$c_{66} = \lim_{u_0\to 0} n_0 \frac{d^2 f_{shear}}{du_0^2}, \tag{28}$$

where $f=F/N_e$ is the deformation energy per electron. The parameters of the distorted lattice for this shear deformation are given by

$$a_0' = a_0, \tag{29a}$$

$$\eta' = \eta\sqrt{1 + u_0 \sin(\varphi)\cos(\varphi) + u_0^2 \sin^2(\varphi)}, \tag{29b}$$

$$\sin(\varphi') = \frac{\sin(\varphi)}{\sqrt{1 + u_0 \sin(\varphi)\cos(\varphi) + u_0^2 \sin^2(\varphi)}}. \tag{29c}$$

(*ii*) *A one-dimensional dilatation along* $\hat{\mathbf{x}}$, *with* $u_x(\mathbf{r})=u_0 x$ *and* $u_y(\mathbf{r})=0$. Here, the strain tensors $e_{x,x}(\mathbf{r})=u_0$, $e_{y,y}(\mathbf{r})=0$, and $e_{x,y}(\mathbf{r})=0$, and the new area of the system is $S'=(1+u_0)S$ and $F_{dx}=\frac{1}{2}Sc_{11}u_0^2$. It then follows that the compression constant c_{11} is given by

$$c_{11} = \lim_{u_0\to 0} n_0 \frac{d^2 f_{dx}}{du_0^2}, \tag{30}$$

while the parameters of the deformed lattice are given by

$$a_0' = a_0, \tag{31a}$$

$$\eta' = \eta\sqrt{1 + (2u_0 + u_0^2)\sin^2(\varphi)}, \tag{31b}$$

$$\sin(\varphi') = \frac{(1+u_0)\sin(\varphi)}{\sqrt{1 + (2u_0 + u_0^2)\sin^2(\varphi)}}. \tag{31c}$$

The surface of the deformed lattice is $S'=a_0'^2\eta' \sin(\varphi')=S(1+u_0)$, so that the filling factor is now given by $\nu'=\nu/(1+u_0)$.

(*iii*) *A one-dimensional dilatation along* $\hat{\mathbf{y}}$ *with* $u_x(\mathbf{r})=0$ *and* $u_y(\mathbf{r})=u_0 y$: Now, the strain tensors $e_{x,x}(\mathbf{r})=0$, $e_{y,y}(\mathbf{r})=u_0$, and $e_{x,y}(\mathbf{r})=0$. The new area of the system is $S'=(1+u_0)S$ and $F_{dy}=\frac{1}{2}Sc_{22}u_0^2$. The compression constant c_{22} is therefore given by

$$c_{22} = \lim_{u_0\to 0} n_0 \frac{d^2 f_{dy}}{du_0^2}. \tag{32}$$

On the other hand, the parameters of the deformed lattice are given by

$$a_0' = (1+u_0)a_0, \tag{33a}$$

$$\eta' = \frac{\eta}{(1+u_0)}\sqrt{1 + (2u_0 + u_0^2)\cos^2(\varphi)}, \tag{33b}$$

$$\cos(\varphi') = \frac{(1+u_0)\cos(\varphi)}{\sqrt{1 + (2u_0 + u_0^2)\cos^2(\varphi)}}. \tag{33c}$$

The surface of the deformed lattice is $S'=a_0'^2\eta' \sin(\varphi')=S(1+u_0)$, so that the filling factor $\nu'=\nu/(1+u_0)$.

(*iv*) *A two-dimensional dilatation with* $u_x(\mathbf{r})=u_0 x$ *and* $u_y(\mathbf{r})=u_0 y$: Now, the strain tensors $e_{x,x}(\mathbf{r})=e_{y,y}(\mathbf{r})=u_0$ and $e_{x,y}(\mathbf{r})=0$. The new area of the system is $S'=(1+u_0)^2S$ and $F_{dxy}=\frac{1}{2}S(c_{11}+2c_{12}+c_{22})u_0^2$. It follows that the combination $c_{11}+2c_{12}+c_{22}$ is given by

$$c_{11}+2c_{12}+c_{22} = \lim_{u_0\to 0} n_0 \frac{d^2 f_{dxy}}{du_0^2}. \tag{34}$$

For this case, there is no need to actually compute the energy of the deformed lattice since we can extract $c_{11}+2c_{12}+c_{22}$ from the Hartree–Fock energy E/N_e given in Eq. (19) in the following manner. The area per electron, s, in the deformed lattice is $s=(1+u_0)^2 s_0$, so that (s_0 here is the area per electron of the undeformed lattice)

$$c_{11}+2c_{12}+c_{22} = 4s_0\left(\frac{d^2 f_{dxy}}{ds^2}\right)_{s=s_0}. \tag{35}$$

The change in s causes a change in the filling factor, which is now given by

$$\nu' = \frac{\nu}{(1+u_0)^2} = \frac{2\pi\ell^2}{s'}. \tag{36}$$

Writing the HF energy as $E/N_e=\left(\frac{e^2}{\kappa\ell}\right)A(\nu)$, we have the relation

$$c_{11}+2c_{12}+c_{22}=\frac{2}{\pi}\left(\frac{e^2}{\kappa\ell^3}\right)\nu^2\left[\nu\frac{d^2A(\nu)}{d\nu^2}+2\frac{dA(\nu)}{d\nu}\right]. \tag{37}$$

Note that the long-wavelength Coulomb term $\frac{2\pi n_0^2 e^2}{\kappa k}$ must be added to c_{11}, c_{12}, and c_{22} that we compute in order to get $\tilde{c}_{11}$, $\tilde{c}_{12}$, and $\tilde{c}_{22}$.

Figure 1 shows the expected quadratic behavior of the deformation energy as a function of u_0 [Eq. (27)] for a shear deformation in the small u_0 limit. In the one- and two-dimensional compressions (i)–(iv), however, Eq. (27) leads to the addition of a nonphysical linear term in the dependence of the energies f_{dx}, f_{dy}, f_{dxy} on u_0, as can be seen in Fig. 2. In the absence of deformation, the average electronic density is equal to that of the positive background. This neutrality removes the divergence of $H(\mathbf{G})$ at $\mathbf{G}=0$ in the Hartree–Fock energy of Eq. (19). When the electron lattice is dilated (but not the positive background), the electronic density no longer matches the density of the positive background and there is a restoring force that arises from this density imbalance. It is easy to show, assuming a density of the form of Eq. (8), that no linear term in u_0 arises when the interaction with the positive background is properly taken into account, and that the interaction with the background does *not* give rise to higher order terms in u_0. Our Hartree–Fock procedure requires that the electronic and background densities be the same even for $u_0\neq 0$, which has the immediate consequence that we cannot directly compute the deformation energy using Eq. (27). For all but the shear deformation, it is thus necessary for us to substract the linear term in Eq. (27) and to add by hand the long-wavelength Coulomb contribution of Eq. (10) in order to get the correct elastic constants. Figure 2 shows that a quadratic behavior for the deformation energy is recovered when the linear term is substracted. Note that the deformation energy in Fig. 2 does not contain the long-wavelength Coulomb contribution of Eq. (10), so that it can be either positive or negative. Our definitions in Eqs. (30), (32), and (34) of the elastic coefficients are not affected by this procedure of removing the linear term in u_0 since they involve the second derivative of the energy with respect to u_0.

It is instructive at this point to note that, for a triangular Wigner crystal of classical electrons, the calculation of Bonsall and Maradudin[14] gives the following expression for the quantity $A(\nu)$

$$A(\nu)=-0.782\,133\sqrt{\nu}, \tag{38}$$

and for the elastic coefficients:

$$c_{12}=-0.108\,92\nu^{3/2}\left(\frac{e^2}{\kappa\ell^3}\right), \tag{39a}$$

$$c_{66}=0.015\,56\nu^{3/2}\left(\frac{e^2}{\kappa\ell^3}\right). \tag{39b}$$

If we use Eq. (37) [with relation (4)] and take c_{66} as given by Eq. (39b), we find $c_{12}=-7c_{66}$, which is consistent with Eq. (39a).

IV. DYNAMICAL MATRIX FROM THE GENERALIZED RANDOM-PHASE APPROXIMATION

We now turn our attention to the calculation of the DM of electron crystals in the GRPA method. In the strong magnetic field limit where the Hilbert space is restricted to one Landau level only, the Hamiltonian of the system is given by

$$H=\sum_{\mathbf{k}}\sum_{\alpha,\beta}u_\alpha(-\mathbf{k})D_{\alpha,\beta}(\mathbf{k})u_\beta(\mathbf{k}), \tag{40}$$

where $\alpha,\beta=x,y$ and $\mathbf{k}$ is a vector restricted to the first Brillouin zone of the crystal. If we define the Matsubara displacement Green's function by

$$G_{\alpha,\beta}(\mathbf{k},\tau)=-\langle T_\tau u_\alpha(\mathbf{k},\tau)u_\beta(-\mathbf{k},0)\rangle, \tag{41}$$

we find, using $\hbar\frac{\partial}{\partial\tau}(\cdots)=[H,(\cdots)]$ and the commutation relation $[u_x(\mathbf{k}),u_y(\mathbf{k}')]=i\ell^2\delta_{\mathbf{k},-\mathbf{k}'}$, that this Green's function is related to the dynamical matrix by

$$G_{\alpha,\beta}(\mathbf{k},i\Omega_n)=\frac{-\ell^4}{\hbar[\Omega_n^2+\omega_{mp}^2(\mathbf{k})]}\begin{pmatrix} D_{y,y}(\mathbf{k}) & -\frac{\hbar\Omega_n}{\ell^2}-D_{x,y}(\mathbf{k}) \\ \frac{\hbar\Omega_n}{\ell^2}-D_{y,x}(\mathbf{k}) & D_{x,x}(\mathbf{k}) \end{pmatrix}_{\alpha\beta}, \tag{42}$$

where $\Omega_n=2\pi n/T$ is a bosonic Matsubara frequency and

$$\omega_{mp}(\mathbf{k})=\frac{\ell^2}{\hbar}\sqrt{\det[D(\mathbf{k})]} \tag{43}$$

is the magnetophonon dispersion relation.

We now define the following density Green's function:

$$\chi^{(\rho,\rho)}_{\mathbf{G},\mathbf{G}'}(\mathbf{k},\tau)=-N_\varphi\langle T_\tau\tilde{\rho}(\mathbf{k}+\mathbf{G},\tau)\tilde{\rho}(-\mathbf{k}-\mathbf{G}',0)\rangle, \tag{44}$$

where $\tilde{\rho}=\rho-\langle\rho\rangle$. In the GRPA, this Green's function is found by solving the following set of equations:[9]

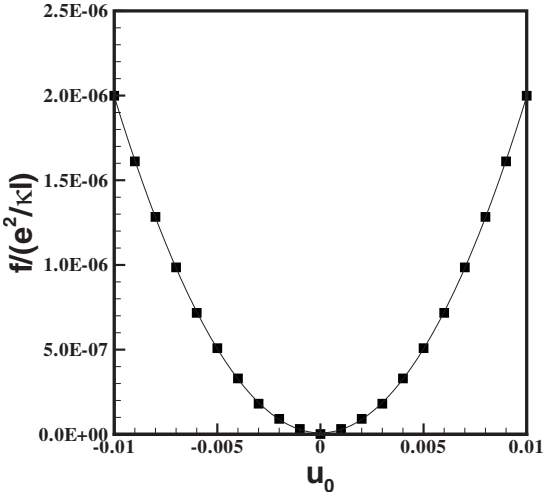

FIG. 1. Deformation energy as a function of u_0 for a shear deformation, $u(\mathbf{r})=u_0 y\hat{\mathbf{x}}$, in a triangular Wigner crystal in Landau level $N=0$ with filling factor $\nu=0.15$. The square symbols are the HFA result, while the solid line is a polynomial fit of order 2 (the linear term is negligible).

$$\sum_{\mathbf{G}''}[i\Omega_n\delta_{\mathbf{G},\mathbf{G}'}-M_{\mathbf{G},\mathbf{G}''}(\mathbf{k})]\chi^{(\rho,\rho)}_{\mathbf{G}'',\mathbf{G}'}(\mathbf{k},i\omega_n)=B_{\mathbf{G},\mathbf{G}'}(\mathbf{q}), \tag{45}$$

with the following definitions:

$$M_{\mathbf{G},\mathbf{G}'}(\mathbf{k})=-2i\left(\frac{e^2}{\hbar\kappa\ell}\right)\langle\rho(\mathbf{G}-\mathbf{G}')\rangle\sin\left[\hat{\mathbf{z}}\cdot\frac{(\mathbf{k}+\mathbf{G})\times(\mathbf{k}+\mathbf{G}')\ell^2}{2}\right][H(\mathbf{G}-\mathbf{G}')-X(\mathbf{G}-\mathbf{G}')-H(\mathbf{k}+\mathbf{G}')+X(\mathbf{k}+\mathbf{G}')] \tag{46}$$

and

$$B_{\mathbf{G},\mathbf{G}'}(\mathbf{k})=2i\langle\rho(\mathbf{G}-\mathbf{G}')\rangle\sin\left[\hat{\mathbf{z}}\cdot\frac{(\mathbf{q}+\mathbf{G})\times(\mathbf{q}+\mathbf{G}')\ell^2}{2}\right]. \tag{47}$$

Diagonalizing the matrix $M(\mathbf{k})$ and making the analytic continuation $i\Omega_n\rightarrow\omega+i\delta$, we can write $\chi^{(\rho,\rho)}_{\mathbf{G},\mathbf{G}'}(\mathbf{k},\omega)$ in the form

$$\chi^{(\rho,\rho)}_{\mathbf{G},\mathbf{G}'}(\mathbf{k},\omega)=\sum_i\frac{W^{(i)}_{\mathbf{G},\mathbf{G}'}(\mathbf{k})}{\omega+i\delta-\tilde{\omega}_i(\mathbf{k})}. \tag{48}$$

At small $\mathbf{k}$, the pole $\tilde{\omega}_i(\mathbf{k})$ with the biggest weight $W^{(i)}_{\mathbf{G},\mathbf{G}}(\mathbf{k})$ gives the GRPA magnetophonon mode. We define this pole as $\tilde{\omega}_{GRPA}(\mathbf{k})$ and the corresponding weight as $W^{(GRPA)}_{\mathbf{G},\mathbf{G}}(\mathbf{k})$.

We now relate the displacement Green's function to the density Green's function using Eq. (9). This last equation, coupled to Eq. (44), gives the following relation between the density and displacement response functions [here, $F(\mathbf{k})$ is the function defined in Eq. (18), where, for simplicity, we now drop the Landau-level index N]:

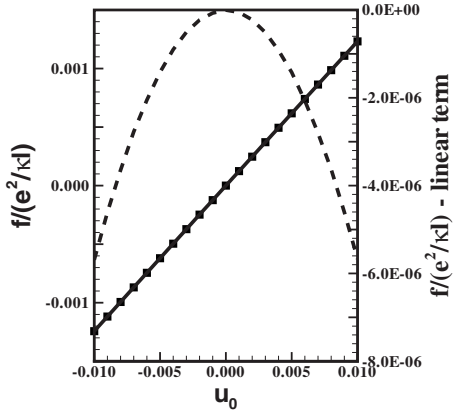

FIG. 2. Deformation energy as a function of u_0 for a one-dimensional dilatation of a triangular Wigner crystal in Landau level $N=0$ with filling factor $\nu=0.15$. The square symbols are the HFA result (left axis), while the solid line is a polynomial fit. The dashed line (right axis) is the deformation energy with the linear term removed.

$$\chi^{(\rho,\rho)}_{\mathbf{G},\mathbf{G}'}(\mathbf{k},\omega)=\nu\frac{h(\mathbf{k}+\mathbf{G})h(\mathbf{k}+\mathbf{G}')}{F(\mathbf{k}+\mathbf{G})F(\mathbf{k}+\mathbf{G}')}\sum_{\alpha,\beta}(k_\alpha+G_\alpha)G_{\alpha,\beta}(\mathbf{k},\omega)\times(k_\beta+G'_\beta). \tag{49}$$

In deriving Eq. (49), we have assumed that $\mathbf{q}\cdot\mathbf{u}(\mathbf{R})\ll 1$, so that a density fluctuation can be linearly related to the displacement $\mathbf{u}(\mathbf{q})$ by Eq. (9). This is equivalent to assuming that the crystal can be described in the harmonic approximation, so that only a knowledge of the dynamical matrix is necessary. To get Eq. (49), we have also assumed that $h(\mathbf{r})=h(-\mathbf{r})$, so that $h(\mathbf{q})$ is real. We can now use Eq. (42) and the symmetry relation $D_{\alpha,\beta}(\mathbf{k})=D_{\beta,\alpha}(\mathbf{k})$ to relate the density response function to the dynamical matrix:

$$\chi^{(\rho,\rho)}_{\mathbf{G},\mathbf{G}'}(\mathbf{k},\omega)=\frac{\nu\ell^4}{\hbar}\frac{\left[\Gamma_1(\mathbf{k})+\frac{i\hbar\omega}{\ell^2}\Gamma_2(\mathbf{k})\right]}{[(\omega+i\delta)^2-\omega^2_{mp}(\mathbf{k})]}\frac{h(\mathbf{k}+\mathbf{G})h(\mathbf{k}+\mathbf{G}')}{F(\mathbf{k}+\mathbf{G})F(\mathbf{k}+\mathbf{G}')}, \tag{50}$$

where we defined

$$\Gamma_1(\mathbf{k})=-\hat{\mathbf{z}}\cdot[(\mathbf{k}+\mathbf{G})\times D(\mathbf{k})\times(\mathbf{k}+\mathbf{G}')]\cdot\hat{\mathbf{z}}, \tag{51a}$$

$$\Gamma_2(\mathbf{k})=\hat{\mathbf{z}}\cdot[(\mathbf{k}+\mathbf{G})\times(\mathbf{k}+\mathbf{G}')]. \tag{51b}$$

For ω close to the magnetophonon resonance, we can write

$$\chi^{(\rho,\rho)}_{\mathbf{G},\mathbf{G}'}(\mathbf{k},\omega)\approx\frac{\nu\ell^4}{\hbar}\frac{Z(\mathbf{k})}{\omega+i\delta-\omega_{mp}(\mathbf{k})}\frac{h(\mathbf{k}+\mathbf{G})h(\mathbf{k}+\mathbf{G}')}{F(\mathbf{k}+\mathbf{G})F(\mathbf{k}+\mathbf{G}')}, \tag{52}$$

where we defined the quantity

$$Z(\mathbf{k})=\frac{\Gamma_1(\mathbf{k})}{2\omega_{mp}(\mathbf{k})}+i\frac{\hbar\Gamma_2(\mathbf{k})}{2\ell^2}. \tag{53}$$

Then, equating Eq. (52) with Eq. (48) for ω close to $\omega_{GRPA}(\mathbf{k})$, we obtain

$$\frac{\nu\ell^4}{\hbar}\frac{Z(\mathbf{k})}{\omega+i\delta-\omega_{mp}(\mathbf{k})}\frac{h(\mathbf{k}+\mathbf{G})h(\mathbf{k}+\mathbf{G}')}{F(\mathbf{k}+\mathbf{G})F(\mathbf{k}+\mathbf{G}')} = \frac{W^{(GRPA)}_{\mathbf{G},\mathbf{G}'}(\mathbf{k})}{\omega+i\delta-\tilde{\omega}_{GRPA}(\mathbf{k})}. \tag{54}$$

Because $\omega_{mp}(\mathbf{k})$ must be equal to $\tilde{\omega}_{GRPA}(\mathbf{k})$, we can finally write

$$\frac{\nu\ell^4}{\hbar}Z(\mathbf{k})\frac{h(\mathbf{k}+\mathbf{G})h(\mathbf{k}+\mathbf{G}')}{F(\mathbf{k}+\mathbf{G})F(\mathbf{k}+\mathbf{G}')} = W^{(GRPA)}_{\mathbf{G},\mathbf{G}'}(\mathbf{k}), \tag{55}$$

or, taking the real and imaginary parts of this equation [we remind the reader that both functions $h(\mathbf{k})$ and $F(\mathbf{k})$ are real]:

$$\mathrm{Re}[W^{(GRPA)}_{\mathbf{G},\mathbf{G}'}(\mathbf{k})] = \frac{\nu}{2}\left[\frac{h(\mathbf{k}+\mathbf{G})h(\mathbf{k}+\mathbf{G}')}{F(\mathbf{k}+\mathbf{G})F(\mathbf{k}+\mathbf{G}')}\right]\frac{\Gamma_1(\mathbf{k})\ell^4}{\hbar\omega_{mp}(\mathbf{k})}, \tag{56a}$$

$$\mathrm{Im}[W^{(GRPA)}_{\mathbf{G},\mathbf{G}'}(\mathbf{k})] = \frac{\nu}{2}\left[\frac{h(\mathbf{k}+\mathbf{G})h(\mathbf{k}+\mathbf{G}')}{F(\mathbf{k}+\mathbf{G})F(\mathbf{k}+\mathbf{G}')}\right]\Gamma_2(\mathbf{k})\ell^2. \tag{56b}$$

We can get rid of the unknown form factors $h(\mathbf{k}+\mathbf{G})$ if we work with the ratio of the imaginary and real parts of the weights. We thus define

$$\Gamma_{\mathbf{G},\mathbf{G}'}(\mathbf{k}) \equiv \frac{\mathrm{Re}[W^{(GRPA)}_{\mathbf{G},\mathbf{G}'}(\mathbf{k})]}{\mathrm{Im}[W^{(GRPA)}_{\mathbf{G},\mathbf{G}'}(\mathbf{k})]},$$

$$= \frac{-\ell^2}{\hbar\omega_{mp}(\mathbf{k})}\frac{(\mathbf{k}+\mathbf{G})\times D(\mathbf{k})\times(\mathbf{k}+\mathbf{G}')}{(\mathbf{k}+\mathbf{G})\times(\mathbf{k}+\mathbf{G}')}. \tag{57}$$

A careful examination shows that, because $\omega_{mp}(\mathbf{k})$ is given by the determinant of the dynamical matrix $D(\mathbf{k})$, the quantity $\Gamma_1(\mathbf{k})/\omega_{mp}(\mathbf{k})$ is unchanged if all the components of the dynamical matrix are multiplied by some constant. Equation (57) is thus indeterminate. To avoid this problem, we replace $\omega_{mp}(\mathbf{k})$ by $\tilde{\omega}_{GRPA}(\mathbf{k})$ in Eq. (57). Our final result is thus

$$\Gamma_{\mathbf{G},\mathbf{G}'}(\mathbf{k}) = \frac{-\ell^2}{\hbar\tilde{\omega}_{GRPA}(\mathbf{k})}\frac{(\mathbf{k}+\mathbf{G})\times D(\mathbf{k})\times(\mathbf{k}+\mathbf{G}')}{(\mathbf{k}+\mathbf{G})\times(\mathbf{k}+\mathbf{G}')}. \tag{58}$$

Because $D_{x,y}(\mathbf{k})=D_{y,x}(\mathbf{k})$, we need to choose three pairs of vectors $(\mathbf{G},\mathbf{G}')$ to get the components of the dynamical matrix. To be valid, the dynamical matrix obtained in this way must satisfy the equation

$$\tilde{\omega}_{GRPA}(\mathbf{k}) = \frac{\ell^2}{\hbar}\sqrt{\det[D(\mathbf{k})]}. \tag{59}$$

Equation (59) provides a check on the validity of our calculation.

V. NUMERICAL RESULTS FOR THE WIGNER CRYSTAL

In this section, we illustrate the application of our method by computing the Lamé coefficients for the triangular Wigner crystal in Landau levels $N=0$ and $N=2$. Figure 3 shows the first two shells of reciprocal lattice vectors of the triangular lattice with $\mathbf{G}_1=(0,0)$. We take the vectors $\mathbf{G}$ and $\mathbf{G}'$ in Eq. (58) on these first two shells. Not all combinations of vectors satisfy Eq. (59). By experimentation, we found that with a combination of the form $[(\mathbf{G},0),(\mathbf{G}',0),(\mathbf{G},\mathbf{G}')]$ with $\mathbf{G},\mathbf{G}'\neq 0$, this equation is satisfied in the irreducible Brillouin zone shown in Fig. 3 to better than 0.05% for $k\ell \lesssim 0.3$. We will thus stick to this type of combination for the rest of this paper.

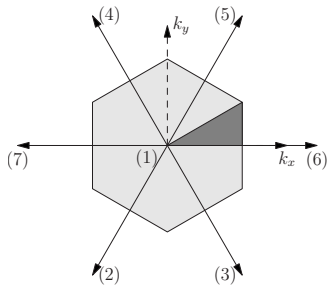

FIG. 3. First Brillouin zone of the triangular lattice with the irreducible Brillouin zone shown as the dark area. The arrows represent the reciprocal lattice vectors on the second shell, while (1) corresponds to the vector $\mathbf{G}=0$.

In the small-wave-vector limit, the dynamical matrix of the Wigner crystal with a triangular lattice structure is given by Eqs. (13a)–(13c). Using Eq. (58), we can extract the elastic coefficients by fitting $D_{\alpha,\beta}(\mathbf{k})$ along the path $k_y=0$, where

$$D_{x,x}(\mathbf{k}) = \left(\frac{e^2}{\kappa\ell^3}\right)\nu k_x\ell + \frac{2\pi}{\nu}(c_{12}+2c_{66})k_x^2\ell^2, \tag{60a}$$

$$D_{x,y}(\mathbf{k}) = 0, \tag{60b}$$

$$D_{y,y}(\mathbf{k}) = \frac{2\pi}{\nu}c_{66}k_x^2\ell^2, \tag{60c}$$

where c_{12} and c_{66} are expressed in units of $e^2/\kappa\ell^3$.

Figure 4 illustrates one limitation of our method: the GRPA dynamical matrix is very much dependent on the choice of the couple $(\mathbf{G},\mathbf{G}')$. Different choices give the same dynamical matrices $D_{\alpha,\beta}(\mathbf{k})$ only in the small-wave-vector limit $k\ell \lesssim 0.1$, as shown in Fig. 4 and, in this limit, the dynamical matrix element $D_{x,x}(\mathbf{k})$ is almost entirely dominated by the long-range Coulomb term [the first term in Eq. (60a)]. It follows that different choices of $(\mathbf{G},\mathbf{G}')$ lead to quite different values of the elastic coefficients c_{12} even though Eq. (59) is satisfied. The coefficient c_{66} obtained from $D_{y,y}(\mathbf{k})$, however, is not affected by the long-range Coulomb interaction and appears to be independent of the choice of $(\mathbf{G},\mathbf{G}')$. Note that the dynamical matrix given by Eq. (58) does not have the correct transformation symmetries of the triangular lattice. In cases where $D_{\alpha,\beta}(\mathbf{k})$ is needed in all the Brillouin zone, it becomes necessary to compute $D_{\alpha,\beta}(\mathbf{k})$ in the irreducible Brillouin zone and obtain $D_{\alpha,\beta}(\mathbf{k})$ in the rest of the Brillouin zone by symmetry.

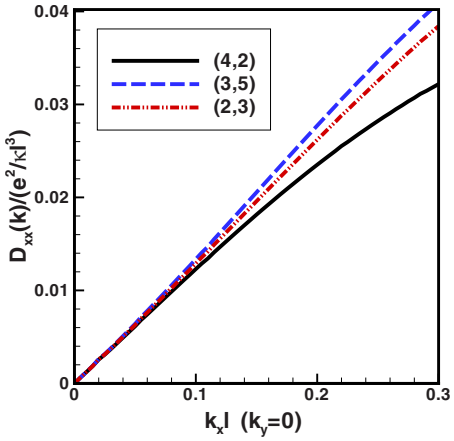

FIG. 4. (Color online) Component $D_{xx}(\mathbf{k})$ of the dynamical matrix along k_x computed for different couples of vectors $(\mathbf{G},\mathbf{G}')$. The numbers in the legend refer to the numeration of the reciprocal lattice vectors shown in Fig. 3.

To give an idea of the variability of the numerical results with $(\mathbf{G},\mathbf{G}')$, we show in Fig. 5 (for N=2) and Fig. 6 (for N=0) the coefficients c_{12} and c_{66} extracted from the GRPA dynamical matrix of the triangular Wigner crystal for different couples of vectors $(\mathbf{G},\mathbf{G}')$. These coefficients are compared with those computed using the HFA described in Sec. III. We show the HFA results by a full line in Figs. 5 and 6. For both N=0 and N=2, we find that the Hartree–Fock results for the coefficient c_{66} are extremely well reproduced by the GRPA method and, as we said above, do not depend on the choice of $(\mathbf{G},\mathbf{G}')$. This is what we expect since the GRPA is the linear response of the crystal about the HFA ground state, so that, taking into account the various approximations made in deriving the GRPA dynamical matrix, the coefficients c_{ij} obtained from the two methods should be roughly equal. In view of Eq. (60c), the coefficient c_{66} is easy to obtain since it is given by a one-parameter fit of the $D_{y,y}(k_x,k_y=0)$ curve. The elastic coefficient c_{12} (which is related to the bulk modulus) is, on the other hand, much more difficult to obtain from Eq. (60a). Indeed, this elastic coefficient turns out to be very sensitive to how accurately the long-wavelength limit $\nu k_x \ell$ of $D_{x,x}(\mathbf{k})$ in Eq. (60a) is obtained by the GRPA numerical calculation. (We note here that the GRPA dynamical matrix *does* contain the long-range Coulomb interaction discussed in Sec. II. The latter does not have to be added by hand, as was the case for the elastic coefficients computed in the HFA.) As we see in Figs. 5(b) and 6(b)), c_{12} is also very sensitive to the choice of the vectors $(\mathbf{G},\mathbf{G}')$ with one particular choice, (2,3), reproducing the HFA results almost exactly. The other two choices give very different values for c_{12}. In the absence of any criteria to choose $(\mathbf{G},\mathbf{G}')$ *a priori*, we would say that the GRPA dynamical matrix cannot be used to make *quantitative* predictions. The *qualitative* behavior of the GRPA elastic coefficient c_{12} is consistent with that of c_{12} computed in the HFA.

If we exclude the domain $\nu \geq 0.19$ where our numerical results become noisy, we find that the average of the GRPA results for the three couples of $(\mathbf{G},\mathbf{G}')$, as shown in Figs. 5(b) and 6(b), are in very good agreement with the HF calculation. In the absence of any criteria to choose the best couple $(\mathbf{G},\mathbf{G}')$, this averaging procedure must be used to get qualitatively and quantitatively reliable results for the GRPA dynamical matrix. For $\nu \geq 0.19$, the crystal softens and the quantum fluctuations in $\mathbf{u}$ are important. There is a transition[10] into a bubble state with two electrons per unit cell at approximately ν=0.22. We do not expect the assumptions underlying our method to be valid in this region.

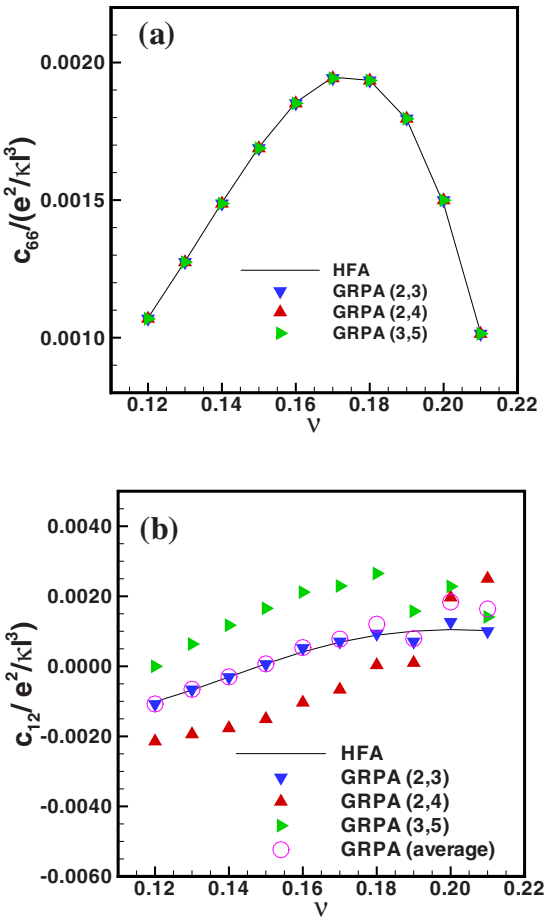

FIG. 5. (Color online) Elastic coefficients (a) c_{66} and (b) c_{12} of the triangular Wigner crystal for Landau level N=2 computed using the different approximations listed in the legend. For the GRPA, the coefficients are computed using three different couples of reciprocal lattice vectors. The numbers in the legend correspond to the numeration of the vectors given in Fig. 3. The empty circles give an average of the three GRPA results. For c_{66}, the different symbols are superimposed.

VI. NUMERICAL RESULTS FOR THE STRIPE CRYSTAL

For the stripe crystal, the dynamical matrix is given by

$$D_{x,x}(\mathbf{k}) = \left(\frac{e^2}{\kappa \ell^3}\right)\frac{\nu}{k\ell}k_x^2\ell^2 + \frac{2\pi}{\nu}(c_{11}k_x^2\ell^2 + c_{66}k_y^2\ell^2 + Kk_y^4\ell^4), \tag{61a}$$

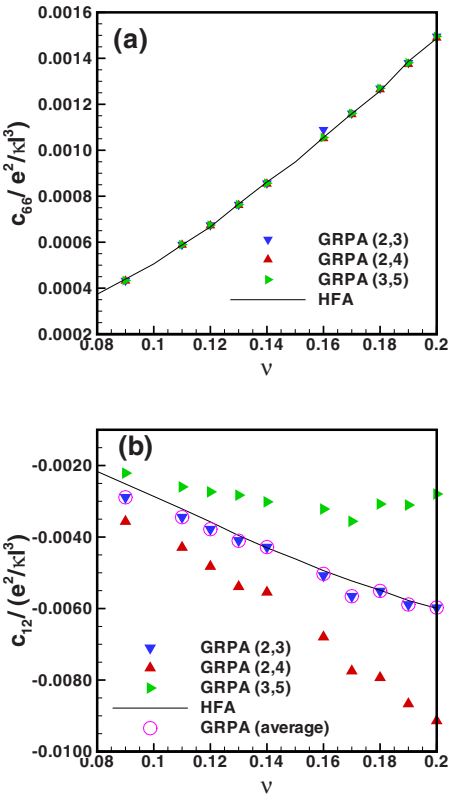

FIG. 6. (Color online) Elastic coefficients (a) c_{66} and (b) c_{12} of the triangular Wigner crystal in Landau level $N=0$ computed in the different approximations indicated in the legend. For the GRPA, the coefficients are computed using three different couples of reciprocal lattice vectors. The numbers in the legend correspond to the numeration of the vectors given in Fig. 3. The empty circles give the average of the three GRPA results. For c_{66}, the different symbols are superimposed.

$$D_{x,y}(\mathbf{k}) = \left(\frac{e^2}{\kappa\ell^3}\right)\frac{\nu}{k\ell}k_x k_y \ell^2 + \frac{2\pi}{\nu}(c_{12}+c_{66})k_x k_y \ell^2, \tag{61b}$$

$$D_{y,y}(\mathbf{k}) = \left(\frac{e^2}{\kappa\ell^3}\right)\frac{\nu}{k\ell}k_y^2 \ell^2 + \frac{2\pi}{\nu}(c_{22}k_y^2 \ell^2 + c_{66}k_x^2 \ell^2), \tag{61c}$$

and the elastic coefficients evaluated in the HFA (Ref. 15) for Landau level $N=2$ are listed in Table I.

TABLE I. Elastic coefficients $n_0^{-1}c_{i,j}$ in units of $e^2/\kappa\ell$ for the stripe crystal at various filling factors and in Landau level $N=2$.

ν	c_{11} $(\times 10^{-2})$	c_{12} $(\times 10^{-1})$	c_{22} $(\times 10^{-2})$	c_{66} $(\times 10^{-5})$
0.42	7.13	−2.43	−0.73	4.35
0.43	5.91	−2.47	−1.15	6.31
0.44	4.95	−2.49	−1.64	7.08
0.45	4.21	−2.50	−2.15	7.10
0.46	3.75	−2.51	−2.65	6.21

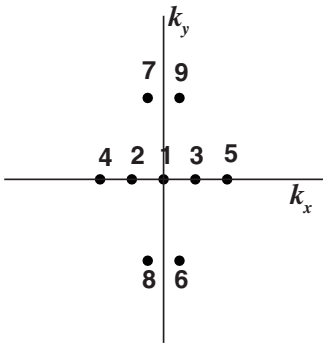

FIG. 7. The first four shells of reciprocal lattice vectors of the anisotropic stripe crystal.

The first four shells of reciprocal lattice vectors of the stripe crystal are represented in Fig. 7. From Eq. (58), the vectors $(\mathbf{G},\mathbf{G}')$ must not be parallel; otherwise, the denominator in this equation vanishes. This forces us to use $\mathbf{G}$ in the second shell and $\mathbf{G}'$ in the fourth shell of reciprocal lattice vectors to evaluate the DM in the GRPA. We show in Figs. 8–10 the elements D_{xx}, D_{xy}, and D_{yy} computed at filling factor $\nu=0.42$ (in Landau level $N=2$) along different directions in $\mathbf{k}$ space together with the corresponding DM in the HFA element obtained from Eqs. (61a)–(61c) with the coefficients of Table I. Similar results are obtained at other filling factors. Notice that the bending coefficient K does not contribute to any of these curves. For each curve, Eq. (59) is perfectly satisfied and the coefficient c_{66}, which can be extracted from the GRPAfunction $D_{yy}(k_x,k_y=0)$, is in excellent agreement with the HFA results given in Table I.

For the GRPA, Figs. 8–10 show results for the couples $(\mathbf{G},\mathbf{G}')$ that produce the maximum and minimum values of the DM element. In all but the $D_{yy}(k_x=0,k_y)$ case, the HFA curve lies between these two results. For $D_{yy}(k_x=0,k_y)$, one of the GRPA curves almost coincides with the HFA result for $k_y\ell \lesssim 0.15$. This is reassuring for the validity of the GRPA

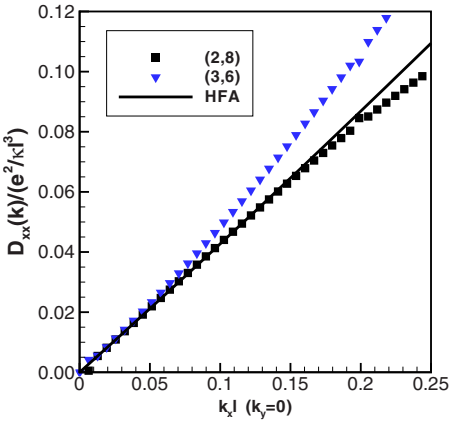

FIG. 8. (Color online) Component $D_{xx}(\mathbf{k})$ of the GRPA and HFA dynamical matrices of the stripe crystal computed along the direction $k_y=0$ for partial filling factor $\nu=0.42$ in Landau level $N=2$, computed using two different couples of reciprocal lattice vectors. The numbers in the legend refer to numbering of the reciprocal lattice vectors in Fig. 7.

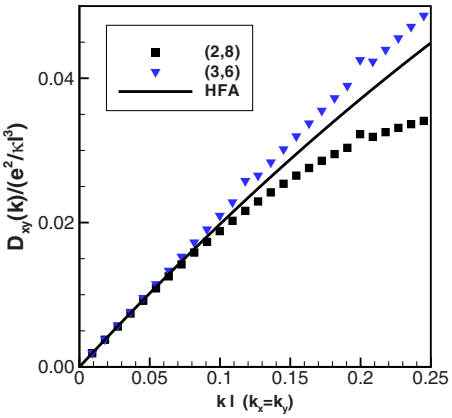

FIG. 9. (Color online) Component $D_{xy}(\mathbf{k})$ of the GRPA and HFA dynamical matrices of the stripe crystal computed along the direction $k_y=k_x$ for partial filling factor $\nu=0.42$ in Landau level $N=2$, computed using two different couples of reciprocal lattice vectors. The numbers in the legend refer to numbering of the reciprocal lattice vectors in Fig. 7.

method, but it also makes it impossible for us to find what part of the difference between the GRPA and HFA is numerical and what part is physical (i.e., due to anharmonicity, for example). We remark that, in the range $k\ell \lesssim 0.15$, the GRPA results are not numerically very different from the small $k\ell$ expansion of the dynamical matrix given in Eqs. (61a)–(61c) with the HFA coefficients. To the credit of our GRPA method, we add that the evolution of the different $D_{i,j}$ with filling factor is consistent with that of the corresponding elements calculated in the HFA, as shown in Fig. 11.

We thus see that the evaluation of the elastic coefficients other than c_{66} from the GRPA results seems hazardous for the stripe crystal. The curvature of the functions D_{xx}, D_{xy}, and D_{yy} in Figs. 8–10 is proportional to c_{11}, $c_{12}+c_{66}$, and c_{22}, respectively. It is clear that the elastic coefficients extracted from these $D_{i,j}$ are much bigger than those obtained from the

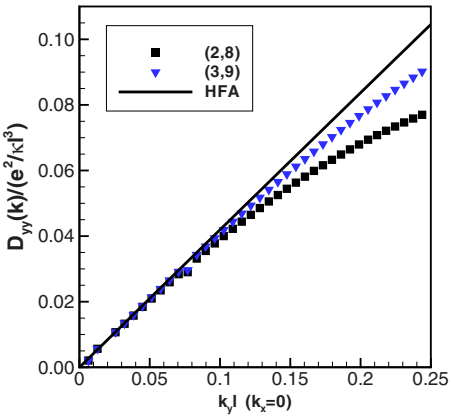

FIG. 10. (Color online) Component $D_{yy}(\mathbf{k})$ of the GRPA and HFA dynamical matrices of the stripe crystal computed along the direction $k_x=0$ for partial filling factor $\nu=0.42$ in Landau level $N=2$, computed using two different couples of reciprocal lattice vectors. The numbers in the legend refer to numbering of the reciprocal lattice vectors in Fig. 7.

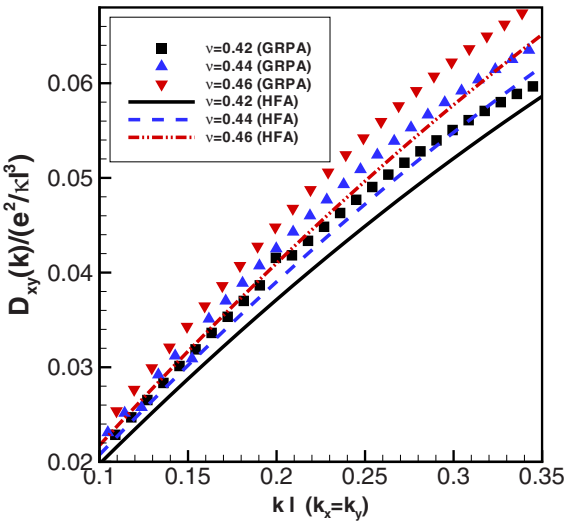

FIG. 11. (Color online) Component $D_{xy}(k)$ of the GRPA and HFA dynamical matrices of the stripe crystal computed along the direction $k_x=k_y$ for different filling factors in Landau level $N=2$.

HFA (the curvature of the HFA function is barely visible in the figures). These coefficients also show very strong variation with the choice of $(\mathbf{G},\mathbf{G}')$. An averaging of the GRPA results for different couples $(\mathbf{G},\mathbf{G}')$ would give a result closer to the HFA but the improvement would not be as dramatic as in the triangular lattice case. In fact, in the case of D_{yy}, we find that averaging over different choices of reciprocal lattice vectors does not bring any improvement to the numerical results.

Finally, we remark that our GRPA results for $D_{xx}(k_x=0,k_y)$ are dominated by a strong k_y^4 behavior, indicating that the bending term K is absolutely essential in the elastic description of the stripe crystal in Eqs. (61a)–(61c).

VII. CONCLUSION

In conclusion, in this paper, we have shown that it is possible to derive an effective dynamical matrix for various crystal states of the 2DEG in a strong magnetic field by computing the density response function in the GRPA. We have compared the dynamical matrix obtained in this way with the one obtained from standard elasticity theory with elastic coefficients computed in the HFA. Our comparison was done for crystals with very different elastic properties, namely, a triangular Wigner crystal and stripe crystal. Our motivation for deriving a dynamical matrix using the GRPA response consists in the fact that the latter has the advantage of giving the dynamical matrix directly without having to compute the elastic coefficients separately. Our comparison with the Hartree–Fock results showed, however, that the GRPA method must be used with care because of the variability of the results with the choice of the couples $(\mathbf{G},\mathbf{G}')$. The shear modulus c_{66} computed in the GRPA agrees very well with the one computed from the HFA, but the values of the other elastic coefficients c_{ij} which are affected by the long-range Coulomb interaction depend very much on the

choice of the couples $(\mathbf{G},\mathbf{G}')$. In some cases, as for a triangular Wigner crystal, an averaging procedure over different couples $(\mathbf{G},\mathbf{G}')$ improves the numerical accuracy of the method. In the long-wavelength $k\ell \ll 1$ limit, however, the GRPA dynamical matrix is a good approximation, both qualitatively and quantitatively, and gives reasonable estimates for the elastic constants of the electronic solids that are in agreement with the static Hartree–Fock calculations.

ACKNOWLEDGMENTS

This work was supported by a research grant (for R.C.) from the Natural Sciences and Engineering Research Council of Canada (NSERC). C.B.D. acknowledges support from NSERC, the Fonds Québécois de Recherche sur la Nature et les Technologies (FQRNT), the Swiss NSF, and the NCCR Nanoscience. Computer time was provided by the Réseau Québécois de Calcul Haute Performance (RQCHP).

[1] P. K. Lam and S. M. Girvin, Phys. Rev. B **30**, 473 (1984); D. Levesque, J. J. Weis, and A. H. MacDonald, *ibid.* **30**, 1056 (1984); K. Esfarjani and S. T. Chui, *ibid.* **42**, 10758 (1990); K. Yang, F. D. M. Haldane, and E. H. Rezayi, *ibid.* **64**, 081301(R) (2001); X. Zhu and S. G. Louie, *ibid.* **52**, 5863 (1995).

[2] For recent reviews, see *Physics of the Electron Solid*, edited by S. T. Chui (International, Boston, 1994), Chap 5; H. Fertig and H. Shayegan, in *Perspectives in Quantum Hall Effects*, edited by S. Das Sarma and A. Pinczuk (Wiley, New York, 1997), Chap. 9.

[3] P. D. Ye, L. W. Engel, D. C. Tsui, R. M. Lewis, L. N. Pfeiffer, and K. West, Phys. Rev. Lett. **89**, 176802 (2002).

[4] Yong P. Chen, G. Sambandamurthy, Z. H. Wang, R. M. Lewis, L. W. Engel, D. C. Tsui, P. D. Ye, L. N. Pfeiffer, and K. W. West, Nat. Phys. **2**, 452 (2006).

[5] Y. P. Chen, R. M. Lewis, L. W. Engel, D. C. Tsui, P. D. Ye, L. N. Pfeiffer, and K. W. West, Phys. Rev. Lett. **91**, 016801 (2003).

[6] R. M. Lewis, Yong Chen, L. W. Engel, D. C. Tsui, P. D. Ye, L. N. Pfeiffer, and K. W. West, Physica E (Amsterdam) **22**, 104 (2004).

[7] R. M. Lewis, P. D. Ye, L. W. Engel, D. C. Tsui, L. N. Pfeiffer, and K. W. West, Phys. Rev. Lett. **89**, 136804 (2002); R. M. Lewis, Y. Chen, L. W. Engel, D. C. Tsui, P. D. Ye, L. N. Pfeiffer, and K. W. West, *ibid.* **93**, 176808 (2004); R. M. Lewis, Yong Chen, L. W. Engel, P. D. Ye, D. C. Tsui, L. N. Pfeiffer, and K. W. West, Physica E (Amsterdam) **22**, 119 (2004).

[8] Yong P. Chen, R. M. Lewis, L. W. Engel, D. C. Tsui, P. D. Ye, Z. H. Wang, L. N. Pfeiffer, and K. W. West, Phys. Rev. Lett. **93**, 206805 (2004).

[9] R. Côté and A. H. MacDonald, Phys. Rev. Lett. **65**, 2662 (1990); Phys. Rev. B **44**, 8759 (1991).

[10] R. Côté, C. B. Doiron, J. Bourassa, and H. A. Fertig, Phys. Rev. B **68**, 155327 (2003); M.-R. Li, H. A. Fertig, R. Côté, and Hangmo Yi, Phys. Rev. Lett. **92**, 186804 (2004); Mei-Rong Li, H. A. Fertig, R. Côté, and Hangmo Yi, Phys. Rev. B **71**, 155312 (2005); R. Côté, Mei-Rong Li, A. Faribault, and H. A. Fertig, *ibid.* **72**, 115344 (2005).

[11] L. D. Landau and E. M. Lifshitz, *Theory of Elasticity* (Oxford, England/Pergamon, New York, 1986).

[12] A. M. Ettouhami, C. B. Doiron, F. D. Klironomos, R. Côté, and Alan T. Dorsey, Phys. Rev. Lett. **96**, 196802 (2006).

[13] A. M. Ettouhami, C. B. Doiron, and R. Côté, Phys. Rev. B **76**, 161306(R) (2007).

[14] L. Bonsall and A. A. Maradudin, Phys. Rev. B **15**, 1959 (1977).

[15] These coefficients were evaluated previously in Refs. 12 and 13. We remark, however, that there was an error in the evaluation of the coefficient c_{12} in Ref. 13 that we have corrected in the present paper. Our previous calculation underestimated the value of c_{12} by a factor of approximately 3. Note also that in the present paper, the stripes are aligned along the y axis, while they were aligned along x in our previous calculation, so that $c_{11} \leftrightarrow c_{22}$.